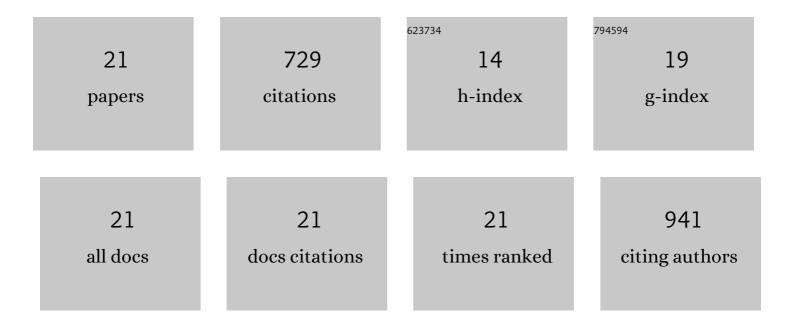
Ting Sun

List of Publications by Year in descending order

Source: https://exaly.com/author-pdf/4142302/publications.pdf Version: 2024-02-01



TINC SUN

#	Article	IF	CITATIONS
1	Maximizing hydrogen production by AB hydrolysis with Pt@cobalt oxide/N,O-rich carbon and alkaline ultrasonic irradiation. Inorganic Chemistry Frontiers, 2022, 9, 2204-2212.	6.0	13
2	Synergistic catalysis of Pd–Ni(OH)2 hybrid anchored on porous carbon for hydrogen evolution from the dehydrogenation of formic acid. International Journal of Hydrogen Energy, 2020, 45, 12849-12858.	7.1	20
3	Mn decorated Na/Fe catalysts for CO ₂ hydrogenation to light olefins. Catalysis Science and Technology, 2019, 9, 456-464.	4.1	96
4	Efficient hydrogen evolution from ammonia borane hydrolysis with Rh decorated on phosphorus-doped carbon. International Journal of Hydrogen Energy, 2019, 44, 16548-16556.	7.1	38
5	Effect of Na Promoter on Fe-Based Catalyst for CO ₂ Hydrogenation to Alkenes. ACS Sustainable Chemistry and Engineering, 2019, 7, 925-932.	6.7	117
6	Nitrogen-Doped Carbon-Stabilized Ru Nanoclusters as Excellent Catalysts for Hydrogen Production. ACS Sustainable Chemistry and Engineering, 2019, 7, 1178-1184.	6.7	65
7	Magnetic, recyclable Pt _y Co _{1â^'y} /Ti ₃ C ₂ X ₂ (X = O, F) catalyst: a facile synthesis and enhanced catalytic activity for hydrogen generation from the hydrolysis of ammonia borane. New Journal of Chemistry, 2017, 41, 2793-2799.	2.8	61
8	Promoted effect of alkalization on the catalytic performance of Rh/alk-Ti 3 C 2 X 2 (X O, F) for the hydrodechlorination of chlorophenols in base-free aqueous medium. Applied Catalysis B: Environmental, 2017, 210, 462-469.	20.2	77
9	Tunable magnetic pole inversion in multiferroic BiFeO ₃ –DyFeO ₃ solid solution. Journal of Materials Chemistry C, 2017, 5, 4063-4067.	5.5	12
10	Brush Scrubbing for Post-CMP Cleaning. , 2017, , 109-133.		1
11	Removal of linear and monobranched alkane from aviation gasoline by 5A zeolite adsorption for octane number enhancement. Canadian Journal of Chemical Engineering, 2016, 94, 128-133.	1.7	8
12	Highly selective gas sensing properties of partially inversed spinel zinc ferrite towards H2S. Sensors and Actuators B: Chemical, 2016, 235, 258-262.	7.8	53
13	Phase transition, piezoelectric, and multiferroic properties of La(Co _{0.5} Mn _{0.5})O ₃ -modified BiFeO ₃ -BaTiO ₃ lead-free ceramics. Physica Status Solidi (A) Applications and Materials Science. 2015. 212. 2012-2022.	1.8	15
14	Improved piezoelectric and bright up-conversion photoluminescent properties in Ho-doped Bi0.5Na0.5TiO3–BaTiO3 lead-free ceramics. Journal of Materials Science: Materials in Electronics, 2015, 26, 6979-6985.	2.2	8
15	Investigation of eccentric PVA brush behaviors in post-Cu CMP cleaning. Microelectronic Engineering, 2012, 100, 20-24.	2.4	25
16	Investigating the effect of diamond size and conditioning force on chemical mechanical planarization pad topography. Microelectronic Engineering, 2010, 87, 553-559.	2.4	40
17	Investigating Effect of Conditioner Aggressiveness on Removal Rate during Interlayer Dielectric Chemical Mechanical Planarization through Confocal Microscopy and Dual Emission Ultraviolet-Enhanced Fluorescence Imaging. Japanese Journal of Applied Physics, 2010, 49, 026501.	1.5	31
18	Optical and Mechanical Characterization of Chemical Mechanical Planarization Pad Surfaces. Japanese Journal of Applied Physics, 2010, 49, 046501.	1.5	20

TING SUN

#	Article	IF	CITATIONS
19	Frictional Analysis of Various Poly(vinyl alcohol) Brush Roller Designs for Post-Interlevel Dielectric CMP Scrubbing Applications. Electrochemical and Solid-State Letters, 2009, 12, H84.	2.2	17
20	Method for Determining the Lubrication Mechanism of Post-ILD CMP Brush Scrubbing. Electrochemical and Solid-State Letters, 2008, 11, H214.	2.2	4
21	Effect of Various Cleaning Solutions and Brush Scrubber Kinematics on the Frictional Attributes of Post Copper CMP Cleaning Process. Solid State Phenomena, 0, 145-146, 363-366.	0.3	8